Weak Epitaxy Growth of Copper Hexadecafluorophthalocyanine (F16CuPc) on p-Sexiphenyl Monolayer Film

ARTICLE *in* THE JOURNAL OF PHYSICAL CHEMISTRY B · FEBRUARY 2009

Impact Factor: 3.3 · DOI: 10.1021/jp8080639 · Source: PubMed

Weak Epitaxy Growth of Copper Hexadecafluorophthalocyanine ($F_{16}CuPc$) on *p*-Sexiphenyl Monolayer Film

Tong Wang,[†] Daniel Ebeling,[‡] Junliang Yang,[†] Chuan Du,[‡] Lifeng Chi,[‡] Harald Fuchs,[‡] and Donghang Yan*,[†]

State Key Laboratory of Polymer Physics and Chemistry, Changchun Institute of Applied Chemistry, Chinese Academy of Sciences, and Graduate School of Chinese Academy of Sciences, Changchun 130022, People's Republic of China, and Physikalisches Institut, Westfälische Wilhelms-Universität, Wilhelm-Klemm-Str. 10, and Center for Nanotechnology (CeNTech), Heisenbergstr. 11, 48149 Münster, Germany

Received: September 11, 2008; Revised Manuscript Received: December 16, 2008

Weak epitaxy growth (WEG) behavior and mechanism of copper hexadecafluorophthalocyanine ($F_{16}CuPc$) on *p*-sexiphenyl (*p*-6P) monolayer film were investigated by atomic force microscopy (AFM), selected area electron diffraction (SEAD), and wide-angle X-ray diffraction (WAXD). High-quality $F_{16}CuPc$ films with high order, large size, and molecular-level smoothness were obtained successfully by WEG method. It was identified that there exists incommensurate epitaxial relation between highly oriented $F_{16}CuPc$ and *p*-6P films. The geometrical channels of *p*-6P monolayer surface induce the nucleation and growth of $F_{16}CuPc$ molecules. Two kinds of in-plane structures, referred to as "phase I" and "phase II", coexist in the initial few molecular layers. As thin-film thickness increases, the distance of (001) plane diminishes and phase I disappears. Furthermore, coalescence, dislocation, and high-angle grain boundary between $F_{16}CuPc$ neighboring domains were observed by high-resolution AFM.

1. Introduction

More attention is being paid to organic thin films due to their considerable promise in organic electronic and optoelectronic devices with recommendable flexibility and modifying properties.[1,2] The morphology and crystal quality of organic thin film dominate the performance of organic electronic devices.[3] Highly ordered, large-size, and continuous organic semiconductor films are advantageous for charge transport in electronic devices.[4] Most organic semiconductors show p-type behavior, while n-type properties are found in only a few materials.[1,5] Especially, some of the n-type materials are unstable in air conditions. However, the n-type semiconductors play important roles on p−n junction diodes, bipolar transistors, complementary circuit, etc. Copper hexadecafluorophthalocyanine ($F_{16}CuPc$) is one of the few promising n-type candidates as air-stable and high-mobility organic semiconductor materials.[5] During the past years, enormous efforts have been made to investigate the growth of $F_{16}CuPc$ thin film on different substrates, such as SiO_2, Al_2O_3, pentacene, etc. for the purpose of improving thin-film quality and further increasing electronic mobility.[6−12] Recently, weak epitaxy growth (WEG) was developed and succeeded in fabricating high-quality organic semiconductor thin films. As a new method, weak epitaxy growth was well suited to fabricate highly oriented film of disklike semiconductor molecules such as phthalocyanine compounds. "Weak" means to decrease the interaction between the molecules and the substrate by way of introducing a new substrate and elevating substrate temperature. Thus, phthalocyanine molecules are upright on the substrate and the $\pi-\pi$ conjugated direction is parallel to the film plane. It is different from conventional OMBE film in which molecules tend to lie flat on the substrate due to the strong interaction between molecules and substrate. Therefore, the WEG is conducive to the carrier transport in the film plane. By the WEG method, the mobility of the organic electronic device with phthalocyanine on *p*-sexiphenyl (*p*-6P) as active layer achieved the same level as the corresponding single crystals.[13,14] The electron mobility of $F_{16}CuPc$ grown on *p*-6P was also achieved as high as 0.11 $cm^2/(V\ s)$.[13] Although the WEG behavior and mechanism of the family of p-type planar phthalocyanines on *p*-6P have been systematically investigated,[15,16] the growth mechanism of $F_{16}CuPc$ on *p*-6P was ambiguous because it exhibits different WEG behavior to that of p-type planar phthalocyanines.

In this work, we report the WEG behavior and mechanism of $F_{16}CuPc$ grown on *p*-6P monolayer. Especially, the first-layer's growth of epitaxial $F_{16}CuPc$ film was investigated in detail. To our knowledge, it is the first time that high-quality $F_{16}CuPc$ films with high order, large size, and molecular-level smoothness were obtained. It provides a potential applied prospect in optoelectronic devices, such as organic field effect transistor (OFET), organic solar cells, organic superlattice, and so on. We performed atomic force microscopy (AFM), selected area electron diffraction (SEAD), and wide-angle X-ray diffraction (WAXD) for investigating the epitaxial relations between highly oriented $F_{16}CuPc$ and *p*-6P films. Four sets of in-plane orientations of incommensurate epitaxy were identified. Two kinds of different in-plane structures, referred to as "phase I" and "phase II", coexist in the initial two or three molecule layers. Furthermore, high-resolution AFM images of seven molecule layers $F_{16}CuPc$ grown on *p*-6P film also showed the phase II. Meanwhile, dislocation and large-angle boundary were observed between neighboring domains.

2. Experimental Section

2.1. Fabrication of Organic Films. The$F_{16}CuPc$ was purchased from Aldrich Co. (USA), and the *p*-6P was synthesized

* Corresponding author. E-mail: yandh@ciac.jl.cn. Fax: +86-431-85262266. Tel.: +86-431-85262165.
[†] Chinese Academy of Sciences.
[‡] Westfälische Wilhelms-Universität and Center for Nanotechnology (CeNTech).

10.1021/jp8080639 CCC: $40.75
Published on Web 01/29/2009

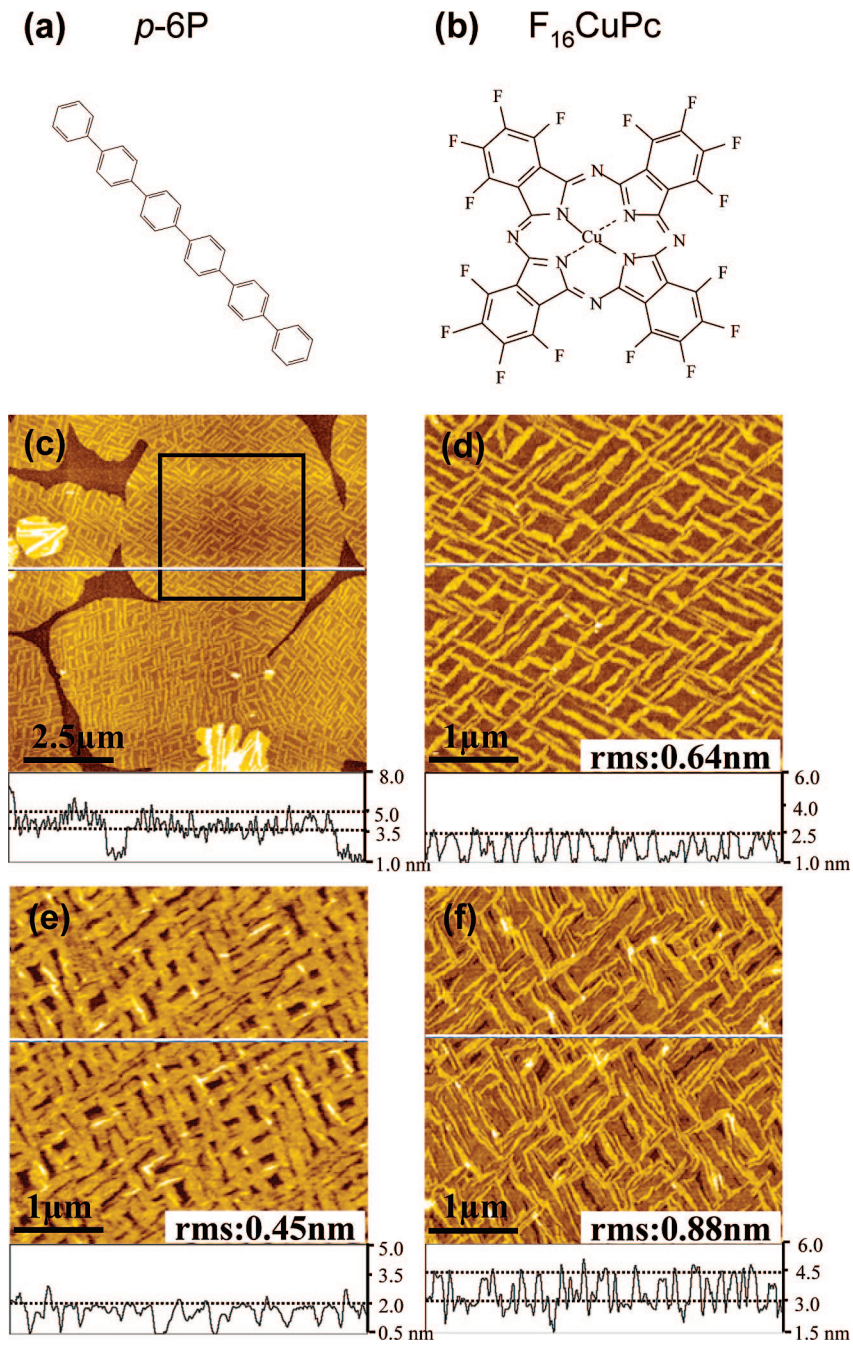

Figure 1. (a and b) Molecular structures of $F_{16}CuPc$ and *p*-6P, respectively. AFM height images of (c and d) 0.5 ML, (e) 0.9 ML, and (f) 2.2 ML $F_{16}CuPc$ grown on *p*-6P monolayer at the substrate temperature of 180 °C. The height data of $F_{16}CuPc$ films shown under each figure correspond to the white lines indicated in the figures. The image in (d) is collected over the square region in (c)

.

according to ref 17. They were purified twice by thermal gradient sublimation prior to experiments. First, 2.5 nm *p*-6P films were deposited on SiO_2 substrate (150 nm thermal oxidation SiO_2 layer on silicon wafer). Then, $F_{16}CuPc$ thin films with different thickness were deposited on *p*-6P thin film. The thin films were deposited under pressure of $10^{-4}-10^{-5}$ Pa at a rate of about 1 nm/min, and the substrate temperature was kept at 180 °C. The conditions and technique are identical for preparation of all organic films.

2.2. Characterization of Organic Films. ***AFM Measurements.*** AFM height images were obtained by a SPI 3800N (Seiko Instruments Inc.) with tapping mode. A 150 μm scanner and a commercially available SiN_4 cantilever with a spring constant of 2 N/m were used in all experiments. High-resolution AFM images were obtained by a Digital Instruments NanoScope IIIa Multimode AFM instrument in contact mode. A 1.5 μm scanner and the BS-SiNi cantilever from BudgetSensors with a smaller spring constant of 0.06 N/m were used. The friction images were used for observation.

TEM Measurements. The organic films of $F_{16}CuPc$/*p*-6P were first deposited on SiO_2 substrate, and then deposited a carbon film on $F_{16}CuPc$/*p*-6P, which is used as support layer. The films were separated from SiO_2 surface by flotation in 10% HF solution. The organic film with the carbon coating was transferred to a copper grid for measurement. The selected area electron diffraction was imaged with a JEOL JEM-1011 transmission electron microscope operated at 100 kV. In order to provide weaker-intensity beam and higher contrast, dark field

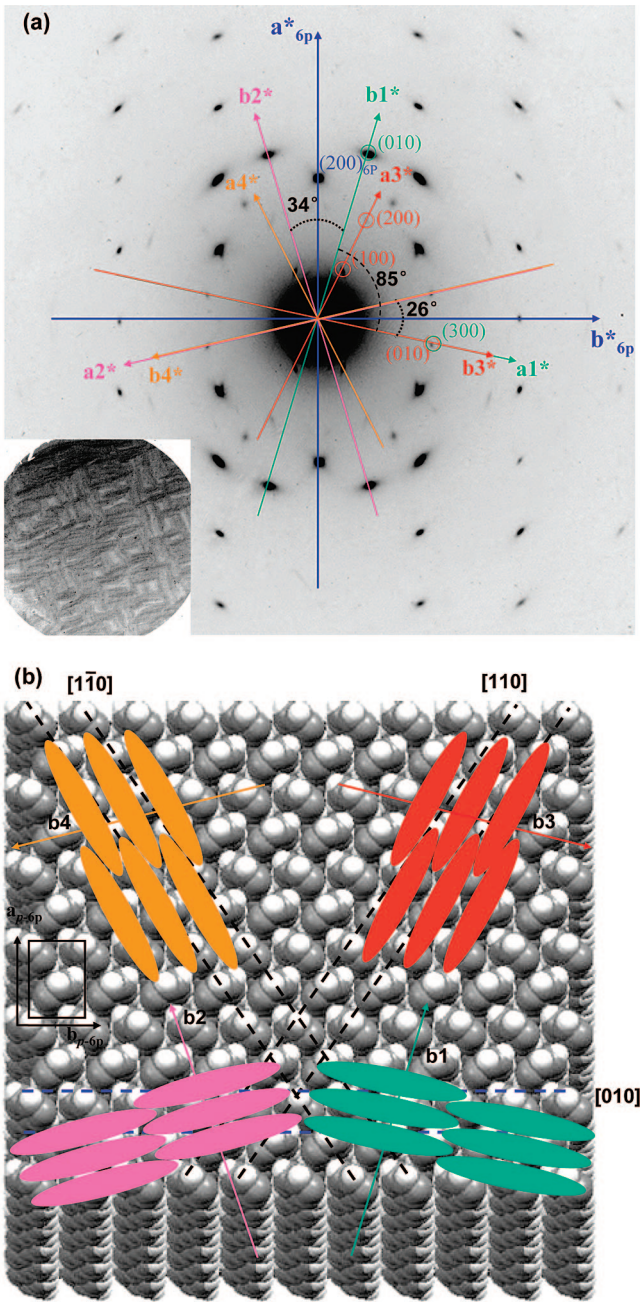

Figure 2. (a) SEAD pattern of 2.2 ML F_{16}CuPc grown on *p*-6P monolayer film. Four sets of in-plane oriented axes are denoted. The inset is the corresponding TEM dark field image. (b) Top view of the schematic diagram of F_{16}CuPc grown on *p*-6P monolayer. Molecule clusters of phase I arrange along the geometrical [010] directions, while molecule clusters of phase II arrange along geometrical channels [110] and [1$\bar{1}$0].

was used for experiment. Simultaneously, MoO_3 was used to calibrate the rotation angle of the image relative to the diffraction pattern.

XRD Measurements. Wide-angle X-ray diffraction was performed in a D8 Discover thin-film diffractometer with Cu Kα radiation (λ = 1.540 56 Å). The scanning rate was 1°/min from 2° to 30°. The selected voltage and current were 40 kV and 40 mA, respectively.

3. Results and Discussion

The molecular structures of sticklike *p*-6P and disklike F_{16}CuPc are given in Figure 1. The liquid-crystal-like *p*-6P monolayer film with large-size domains is used as epitaxial substrate.[18,19] Figure 1c−f shows the morphologies of F_{16}CuPc grown on *p*-6P monolayer film with different thicknesses. According to Figure 1c, we can observe several *p*-6P monolayer domains on the SiO_2 substrate. Meanwhile, the height data show that about 2.5 nm between the bottom (1.0 nm) and the adjacent dashed (3.5nm) is the thickness of *p*-6P monolayer film approximately. And then 0.5 molecule layer (0.5 ML) F_{16}CuPc was grown on these large-size *p*-6P monolayer domains. The needlelike F_{16}CuPc crystals present two in-plane orientations and form many parallelograms, as shown in Figure 1d which is collected over the square region in Figure 1c. The angle between two oriented directions is about 85°. The average single domain size of F_{16}CuPc film can reach at 0.6−1.0 μm. The height data of F_{16}CuPc films shown under each figure are corresponding to the white lines. Each molecule layer of F_{16}CuPc films is about 1.5 nm, which is approximately equal to the molecule dimension. Hence, similarly to the family of p-type phthalocynines, F_{16}CuPc molecules are approximately standing-up on the *p*-6P monolayer film.[13,15,16] Figure 1e is about 0.9 ML F_{16}CuPc on monolayer *p*-6P film with dense intertexture-shape islands. With F_{16}CuPc thickness increasing, the intertexture-shape islands continue to close and adjacent domains come to coalesce, as shown in Figure 1f (about 2.2 ML). The third molecule layer emerges almost after the second molecule layer has coalesced completely. It suggests that F_{16}CuPc growth is the layer-by-layer mode, i.e., Frank van der Merwe mode, on monolayer *p*-6P film at the early stages. Consequently, the F_{16}CuPc films are very smooth and the root-mean-square (rms) roughness is less than 1 nm. These smooth F_{16}CuPc films are very important and useful, because the quality of the initial few layers determines not only the subsequent film growth but also the charge transport.[20−22]

TABLE 1: In-plane Parameters of *p*-6P Monolayer and F_{16}CuPc Film Grown on *p*-6P Monolayer Film

	p-6P (monolayer)[a]	F_{16}CuPc (phase I)[b]	F_{16}CuPc (phase II)[b]
$d_{(100)}$ (Å)	7.84	14.61 ± 0.04	10.21 ± 0.03
$d_{(010)}$ (Å)	5.59	3.20 ± 0.02	4.87 ± 0.02
γ (deg)	90	85 ± 0.5	75 ± 0.5

[a] From ref 15. [b] Taken from average values measured in SEAD patterns.

The experiments of selected area electron diffraction (SAED) are performed to study the epitaxial relations between F_{16}CuPc and the *p*-6P substrate. Figure 2a is SAED pattern of 2.2 ML F_{16}CuPc grown on *p*-6P monolayer film. The indexed ED pattern shows it consists of one [001] zone of *p*-6P and four [001] zones of F_{16}CuPc. There coexist two kinds of in-plane structures of F_{16}CuPc referred to as "phase I" and "phase II", which are somewhat different from the reported parameters.[10] After calculating statistically and demarcating with gold, the in-plane parameters of *p*-6P monolayer and F_{16}CuPc films can be obtained, and they are summarized in Table 1. Four sets of in-plane orientations of incommensurate epitaxy were revealed by indexed ED pattern. For phase I, there are two symmetrical oriented relations that there is an angle of about ±17° between the b*-axis (corresponding b1* and b2* denoted in Figure 2a) of F_{16}CuPc and the a*-axis of the *p*-6P. For phase II, there are also two symmetrical oriented relations that there is an angle of about ±13° between the b*-axis (corresponding b3* and b4* denoted in Figure 2a) of F_{16}CuPc and the b*-axis of the *p*-6P. It is worth noting that the angle between the b*-axis of phase I and the b*-axis of phase II is 85°, which is coincident with

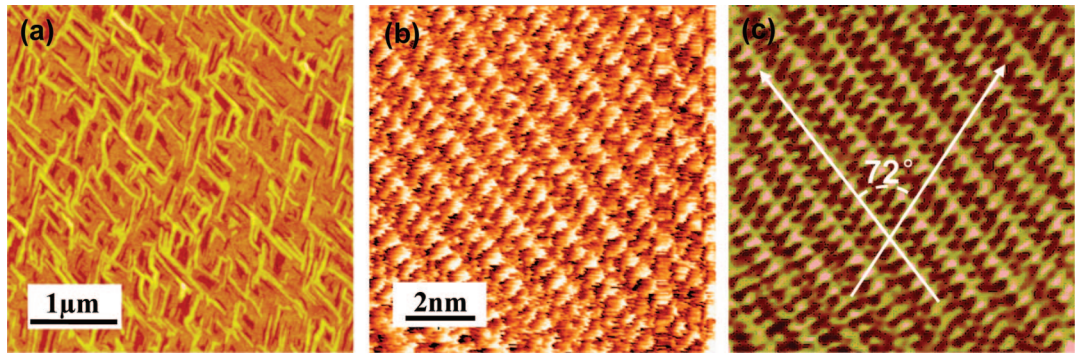

Figure 3. (a) 4 × 4 μm^2 AFM topographic image of 7.0 ML $F_{16}CuPc$ grown on *p*-6P monolayer film. (b, c) High-resolution AFM image of 10 × 10 nm^2 selected regions from (a) and its filtered high-resolution AFM image by Fourier transform.

the angle of two oriented directions in AFM height images (Figure 1). This further confirmed that two phases coexist and grow simultaneously. The crystal grains grow along their b directions which are identical to the direction of $\pi-\pi$ conjugation. Consequently, the grains of different phases grow respectively till they collide and coalesce together. The schematic diagram of $F_{16}CuPc$ grown on *p*-6P monolayer is shown in Figure 2b. The green and pink ellipses represent phase I molecules, while the red and orange ones represent phase II molecules corresponding to the indication in the SAED pattern. Four sets of in-plane orientations of incommensurate epitaxy are closely related to the geometrical channel between the prominent H-atoms of (001) plane of the *p*-6P film. There are three prime geometrical channels along [110], [1$\bar{1}$0], and [010] directions, respectively. The nucleation of initial molecules tends to happen along the channels and rotate to a lowest energy location. Two epitaxial relations of phase I result from nucleating along the [010] channel on (001) plane of *p*-6P film, while the other two epitaxial relations of phase II result from nucleating along the [110] and [1$\bar{1}$0] channels. The molecules nucleate and arrange along the geometrical channels, but not completely parallel to the directions of geometrical channels. The tiny mismatch between the molecules orientations and the geometrical channels was induced by intermolecular $\pi-\pi$ interaction and molecule−substrate vdW force. Therefore, the oriented relations between $F_{16}CuPc$ and the *p*-6P substrate result from the synergism of $\pi-\pi$ interaction of $F_{16}CuPc$ molecules, vdW force, and geometrical channels.[23,24]

The topographic image of 7.0 ML $F_{16}CuPc$ (Figure 3a) is similar to the morphology 2.2 ML $F_{16}CuPc$ (Figure 1f) grown on *p*-6P monolayer film except for the diminishing of the angle between two oriented directions. In order to investigate the morphology and structure of $F_{16}CuPc$ film in detail, high-resolution AFM was carried out by contact mode, as shown in Figure 3b. Well-ordered arrays of molecules emerge in the friction images of 7.0 ML $F_{16}CuPc$ grown on *p*-6P monolayer film. It is evident that the periodic rows in two directions are distinguished from the filtered high-resolution AFM images in Figure 3c. The spacing in periodicity of 11.05 ± 0.03 and 4.84 ± 0.04 Å are identified and the angle between two directions is 72°, as depicted in Figure 3c. These parameters correspond to the above phase II. However, no results corresponding to phase I were observed in many other experiments. Thus, we can deduce that the phase I is the film phase emerging at the initial few molecule layers, while phase II becomes dominant with increasing thickness of $F_{16}CuPc$ film.

Occasionally, some crystal defects such as linear defect and high-angle grain boundary were observed in high-resolution AFM images. Defects come into being from releasing stress

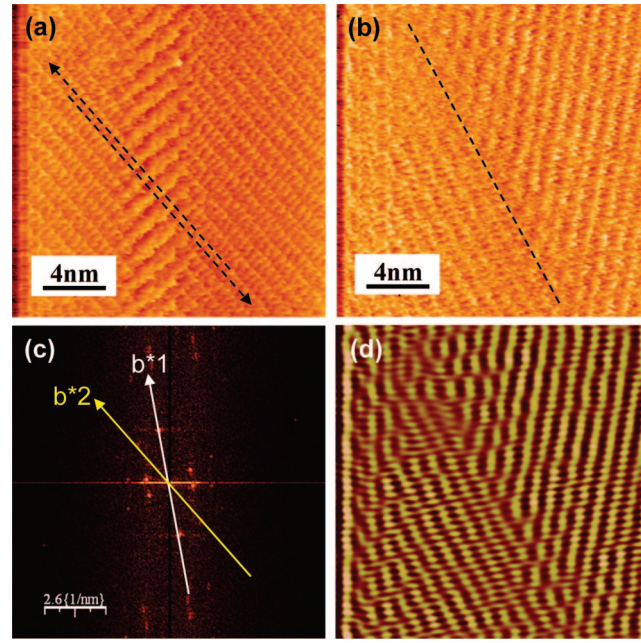

Figure 4. (a) High-resolution AFM image of 7.0 ML $F_{16}CuPc$ grown on *p*-6P monolayer film. The distance between two black parallel lines with arrows denotes the displacement of dislocation. (b) High-resolution AFM image of 7.0 ML $F_{16}CuPc$ grown on *p*-6P monolayer film reveals grain boundary. (c) The corresponding Fourier transform spectra of (b). (d) Filtered AFM images from (b) by Fourier transform.

and maintaining lowest energy spontaneously during the film growth. Figure 4a shows the dislocation feature with the burgers vector displacement of about half-crystal lattice in axis "a" direction (as the distance between two black parallel lines with arrows denoted). In other words, an extra half-plane dislocation exists on the glide plane. This kind of dislocation tends to form at the joint of the two neighboring $F_{16}CuPc$ grains with the same oriented directions. During the film growth, once two parallel crystal clusters or grains along the direction of densely stacking meet, the molecules at the joint will adjust their position to each other in order to suit the changes of intermolecular interaction and potential energy; therefore, some dislocations formed. Furthermore, high-angle grain boundary was observed which is the similar structure and behavior with metals and ceramic materials,[25,26] as shown in Figure 4b. This kind of defect tends to form at the joint of the two neighboring $F_{16}CuPc$ grains with different oriented directions. The oriented angle between two neighboring domains is about 30°. Consequently, dislocations in a row at the interface bring crystal lattice distortion. The higher the density of superposition is, the better the interface connection is, and the lower the grain boundary energy is. On

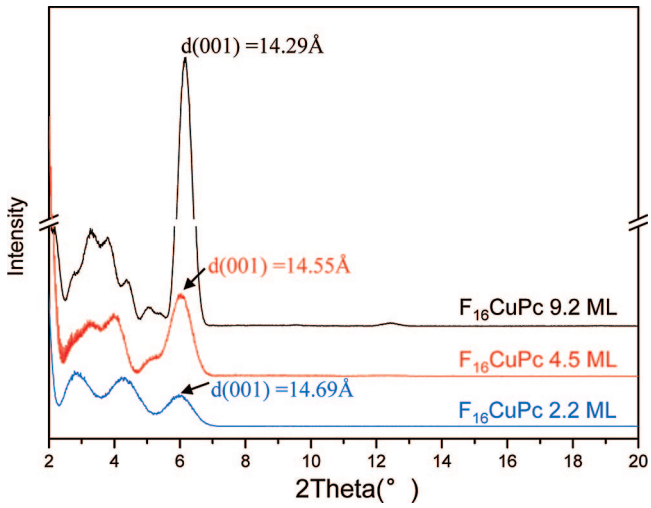

Figure 5. X-ray diffraction data for different thickness $F_{16}CuPc$ grown on *p*-6P monolayer film. The distance between molecule layers becomes smaller from 14.69 to 14.29 Å as the thickness increases.

the one hand, the defects relax the strain coming from film growth, which is beneficial to forming continuous films. On the other hand, defects may result in poor device performance because of trapping of the charge carriers.

Figure 5 shows the X-ray diffraction patterns of $F_{16}CuPc$ grown on 2 nm *p*-6P monolayer film, with $F_{16}CuPc$ thickness ranging from 2.2 to 9.2 ML. The patterns demonstrate that peaks intensity become stronger as the thickness increases. Moreover, the distance between molecule layers changes from 14.69 to 14.29 Å. The obtained layer spacing implies that $F_{16}CuPc$ molecules are standing up on the *p*-6P substrate with some tiny tilt angle. The variation of distance results from the difference on the molecule−substrate interaction and the intermolecular interaction. For instance, the interaction between the first $F_{16}CuPc$ molecular layer and *p*-6P substrate is so weak that it may induce the $F_{16}CuPc$ molecules to be standing up with some tiny tilting angle. However, the interaction between the subsequent $F_{16}CuPc$ molecular layers may be rather a little stronger. Thus, the tilting angles of $F_{16}CuPc$ molecules become a little bigger. Therefore, the distance between layers diminishes along with the thickness of $F_{16}CuPc$ film increasing. On the other hand, the 2.2 ML thick film consists of the mixture of two phases, whereas phase II is dominant in the 9.2 ML thick film. This shift in the XRD peak comes from the difference in the tilting angles for $F_{16}CuPc$ molecules between phase I and phase II, which results from the change of molecule−substrate interaction and intermolecular interaction with increasing thin-film thickness. Hence, it is confirmed that phase transition happens during the films' growth.

4. Conclusions

We investigated weak epitaxy growth (WEG) behavior and mechanism of copper hexadecafluorophthalocyanine ($F_{16}CuPc$) on *p*-sexiphenyl (*p*-6P) monolayer film by atomic force microscopy (AFM), selected area electron diffraction (SEAD), and wide-angle X-ray diffraction (WAXD). The incommensurate epitaxial relations between highly oriented $F_{16}CuPc$ and *p*-6P film were identified. The geometrical channels of *p*-6P monolayer surface induce the nucleation and growth of $F_{16}CuPc$ molecules. Two kinds of different in-plane structures, referred to as phase I and phase II, coexist in the initial few molecule layers. There are two symmetrical oriented relations that there is an angle of about ±17° or ±13° between the b*-axis of $F_{16}CuPc$ and the a*-axis of the *p*-6P or the b*-axis of the *p*-6P. However, as thin-film thickness increases, the distance of the (001) plane decreases and phase I disappears. In other words, only phase II exists in thicker $F_{16}CuPc$ thin films. Furthermore, dislocation and high-angle grain boundary were observed between neighboring grains by high-resolution AFM. Through WEG method, high-quality $F_{16}CuPc$ thin films that exhibit the characteristics of large size, high order, and molecular-level smoothness were fabricated on the epitaxial substrate of *p*-sexiphenyl (*p*-6P) monolayer film, which will have significant application in organic film electronic and optoelectronic devices.

Acknowledgment. This work was financially supported by the National Natural Science Foundation of China (50773079, 20621401).

References and Notes

(1) Horowitz, G. *Adv. Mater.* **1998**, *10*, 365.
(2) Dimitrakopoulos, C. D.; Malenfant, P. R. L. *Adv. Mater.* **2002**, *14*, 99.
(3) Bao, Z.; Lovinger, A. J.; Dodabalapur, A. *Adv. Mater.* **1997**, *9*, 42.
(4) Bao, Z.; Lovinger, A. J.; Dodabalapur, A. *Appl. Phys. Lett.* **1996**, *69*, 11.
(5) Bao, Z.; Lovinger, A. J.; Brown, J. *J. Am. Chem. Soc.* **1998**, *120*, 207.
(6) Ossó, J. O.; Schreiber, F.; Kruppa, V.; Dosch, H.; Garriga, M.; Alonso, M. I.; Cerdeira, F. *Adv. Funct. Mater.* **2002**, *12*, 455.
(7) Ossó, J. O.; Schreiber, F.; Alonso, M. I.; Garriga, M.; Barrena, E.; Dosch, H. *Org. Electron.* **2004**, *5*, 135.
(8) de Oteyza, D. G.; Barrena, E.; Ossó, J. O.; Dosch, H.; Meyer, S.; Pflaum, J. *Appl. Phys. Lett.* **2005**, *87*, 183504.
(9) de Oteyza, D. G.; Barrena, E.; Sellner, S.; Ossó, J. O.; Dosch, H. *J. Phys. Chem. B* **2006**, *110*, 16618.
(10) de Oteyza, D. G.; Barrena, E.; Sellner, S.; Ossó, J. O.; Dosch, H. *J. Am. Chem. Soc.* **2006**, *128*, 15052.
(11) Wakayama, Y. *J. Phys. Chem. C* **2007**, *111*, 2675.
(12) de Oteyza, D. G.; Barrena, E.; Ossó, J. O.; Sellner, S.; Dosch, H. *Chem. Mater.* **2006**, *18*, 4212.
(13) Wang, H.; Zhu, F.; Yang, J.; Geng, Y.; Yan, D. *Adv. Mater.* **2007**, *19*, 2168.
(14) Wang, H.; Song, D.; Yang, J.; Yu, B.; Geng, Y.; Yan, D. *Appl. Phys. Lett.* **2007**, *90*, 253510.
(15) Yang, J.; Wang, T.; Wang, H.; Zhu, F.; Li, G.; Yan, D. *J. Phys. Chem. B* **2007**, *112*, 3132.
(16) Wang, T.; Yang, J.; Wang, H.; Zhu, F.; Yan, D. *J. Phys. Chem. B* **2008**, *112*, 6786.
(17) Garnier, F.; Horowitz, G.; Peng, X. Z. *Synth. Met.* **1991**, *45*, 163.
(18) Yang, J.; Wang, T.; Wang, H.; Zhu, F.; Li, G.; Yan, D. *J. Phys. Chem. B* **2008**, *112*, 7816.
(19) Yang, J.; Wang, T.; Wang, H.; Zhu, F.; Li, G.; Yan, D. *J. Phys. Chem. B* **2008**, *112*, 7821.
(20) Ruiz, R.; Nickel, B.; Koch, N.; Feldman, L. C.; Haglund, R. F., Jr.; Kahn, A.; Family, F.; Scoles, G. *Phys. Rev. Lett.* **2003**, *91*, 136102.
(21) Meyer zu Heringdorf, F. J.; Reuter, M. C.; Tromp, R. M. *Nature* **2001**, *412*, 517.
(22) Dinelli, F.; Murgia, M.; Levy, P.; Cavallini, M.; Biscarini, F. *Phys. Rev. Lett.* **2004**, *92*, 116802.
(23) Campione, M.; Sassella, A.; Moret, M.; Papagni, A.; Trabattoni, S.; Resel, R.; Lengyel, O.; Marcon, V.; Raos, G. *J. Am. Chem. Soc.* **2006**, *128*, 13378.
(24) Marcon, V.; Raos, G.; Campione, M.; Sassella, A. *Crystal Growth Des.* **2006**, *6*, 1826.
(25) Gleiter, H.; Chalmers, B. *Prog. Mater. Sci.* **1972**, *16*, 1.
(26) Wirth, R. *J. Mater. Sci. Lett.* **1986**, *5*, 105.

JP8080639